

parameters were selected as follows: rock density (kg/m^3) =2200; Acceleration of gravity (kg/N) =10; Volume modulus (Pa)=5e10; Shear modulus (Pa)= 1e10; Friction Angle =30°; Cohesion (N)=18e7; Tensile strength (N/m^2) =1e7. The stress applied at the Z=30m plane is $y_h=22000 \times (500-30)=10.34 \times 10^6 \text{N/m}^2$.

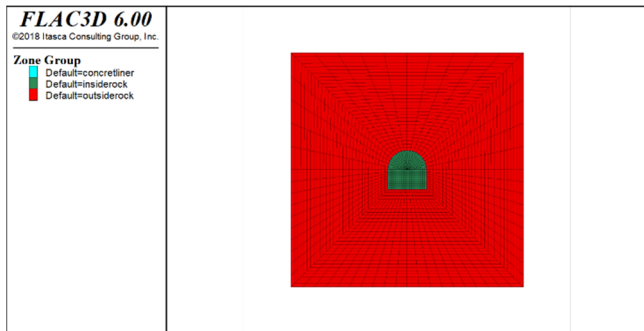


Figure 3. Model of the tunnel when it is not excavated

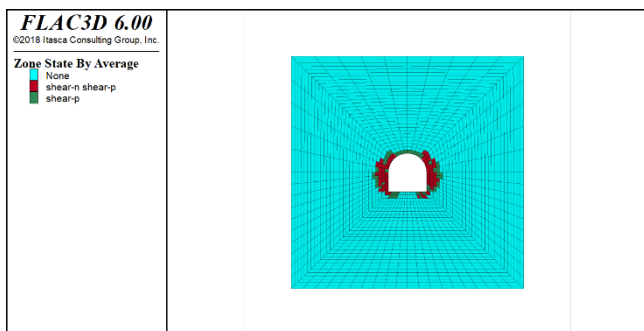


Figure 4. The plastic zone of the cavity after excavation

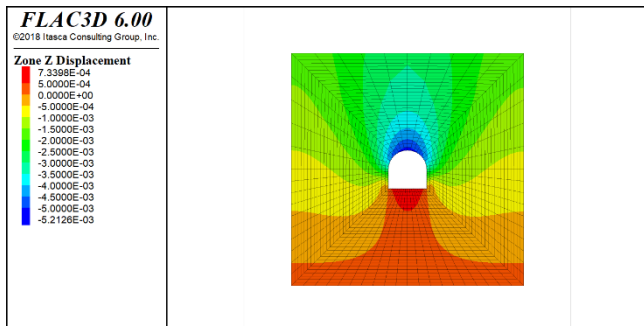


Figure 5. Displacement contour in the Z direction after excavation

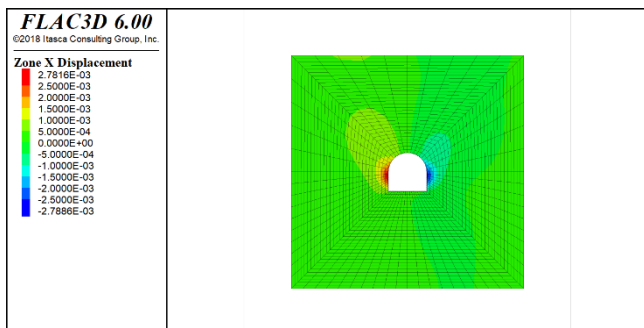


Figure 6. Displacement contour in the X direction after excavation

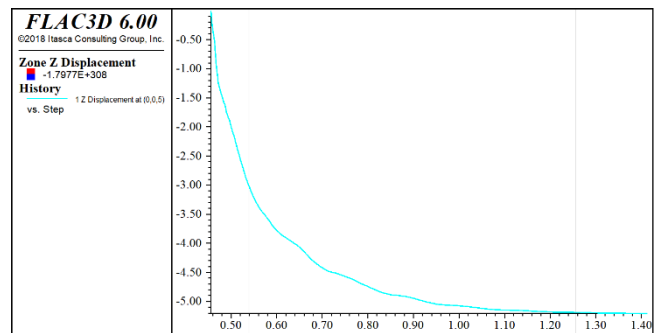


Figure 7. Displacement curve in the Z direction after excavation

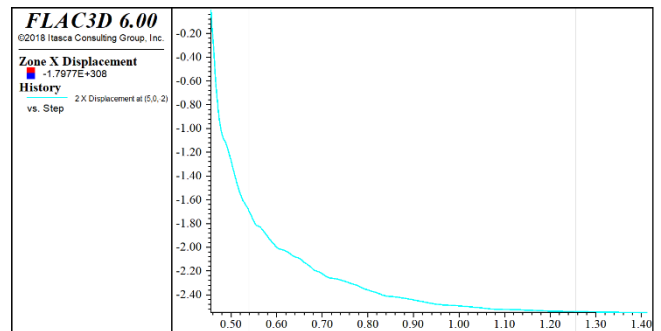


Figure 8. Displacement curve in the X direction after excavation

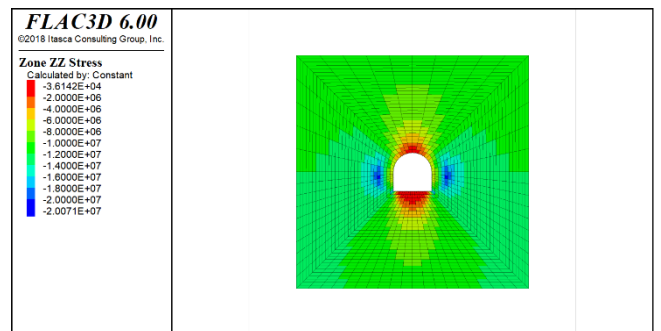


Figure 9. Stress in the Z direction after excavation

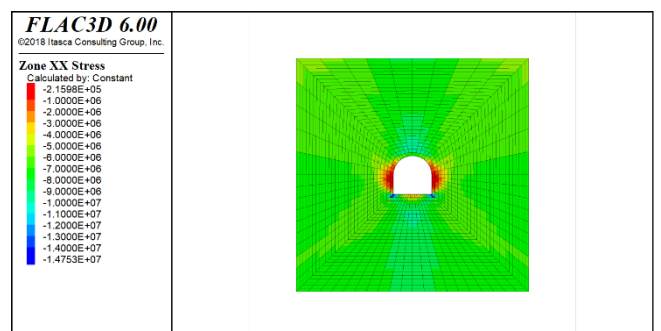


Figure 10. Stress in the X direction after excavation

It can be seen that the vault sinks 4.775mm without support after excavation, the horizontal convergence of the side wall is 2.996mm, and the plastic zone of the surrounding rock is shown in the figure above.

4. The Influence of Side Pressure Coefficient

The plastic zones after excavation with different side pressure coefficients are shown in the figure below:

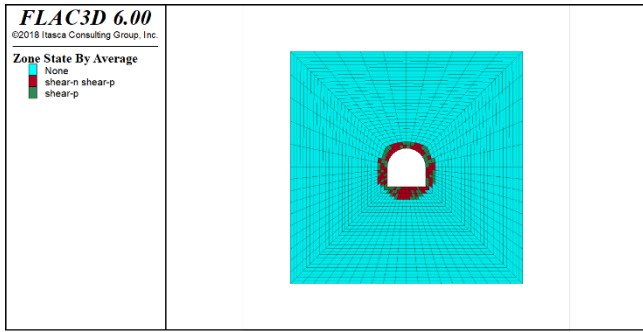


Figure 11. $\lambda=0.5$

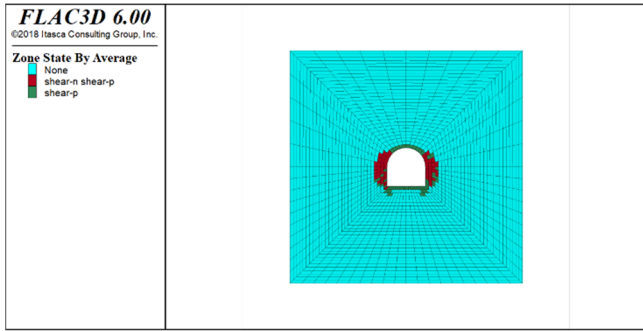


Figure 12. $\lambda=1$

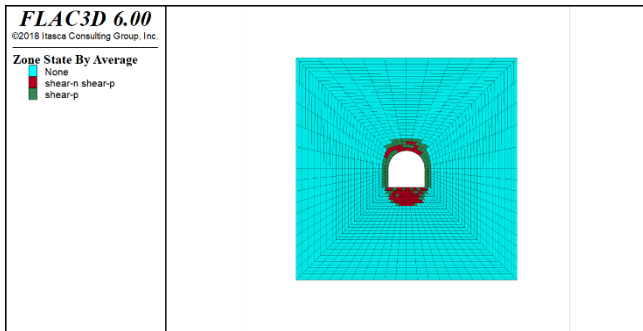


Figure 13. $\lambda=1.5$

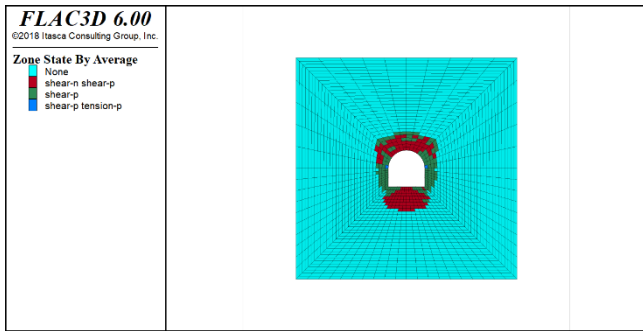


Figure 14. $\lambda=2$

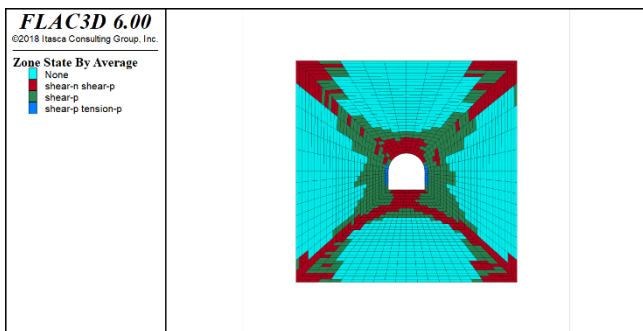


Figure 15. $\lambda=2.5$

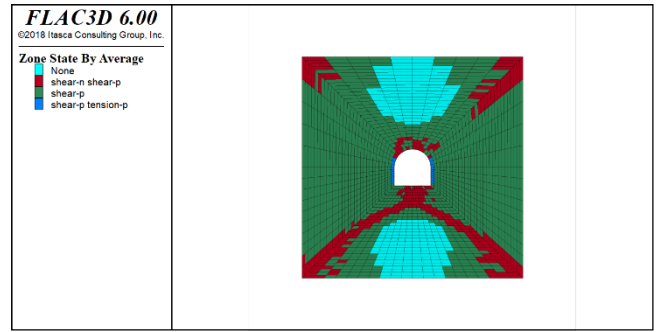


Figure 16. $\lambda=3$

With the increase of the lateral pressure coefficient, the plastic zone of the tunnel top and the side wall is gradually increasing, and the vault expands more, when the lateral pressure coefficient is 2.5, the plastic zone expands sharply and cannot be self-stable.

The displacement contours in the Z direction after excavation with different lateral pressure coefficients are shown in the figure below:

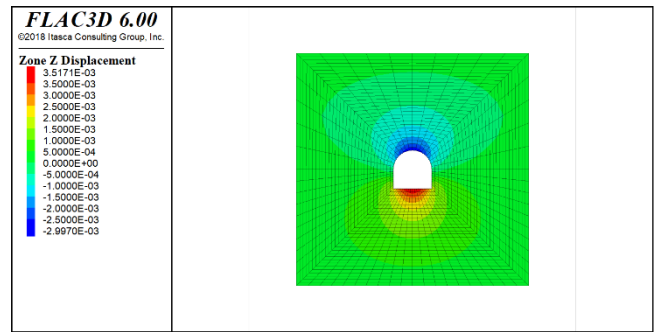


Figure 17. $\lambda=1.5$

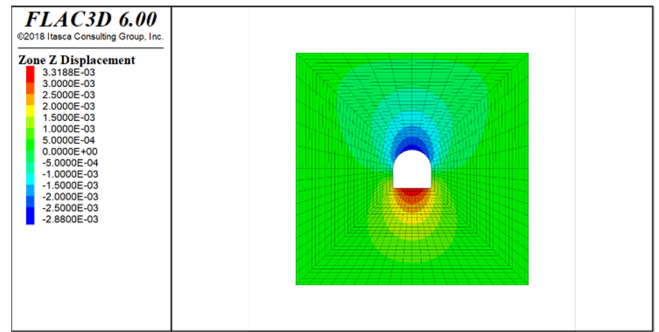


Figure 18. $\lambda=2$

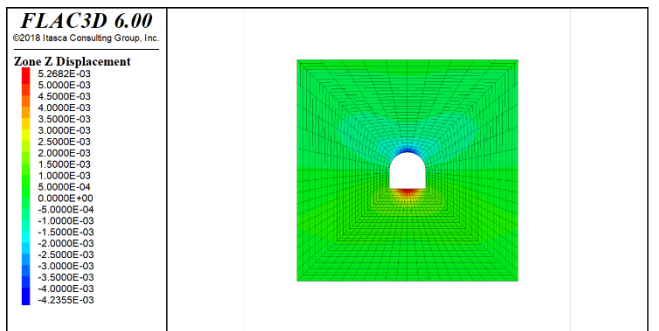


Figure 19. $\lambda=1.5$

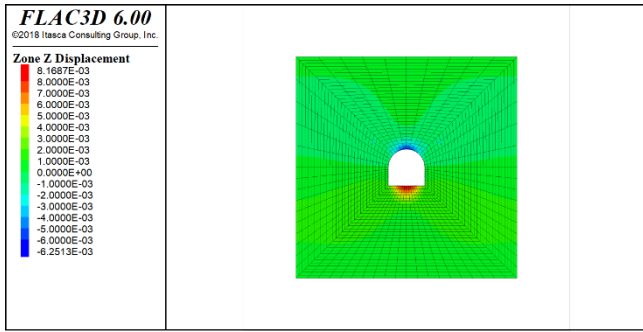


Figure 20. $\lambda=2$

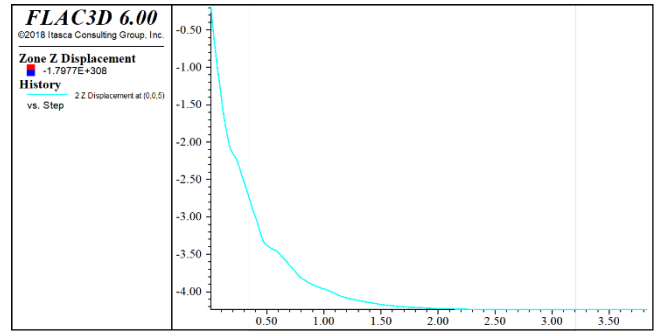


Figure 25. $\lambda=1.5$

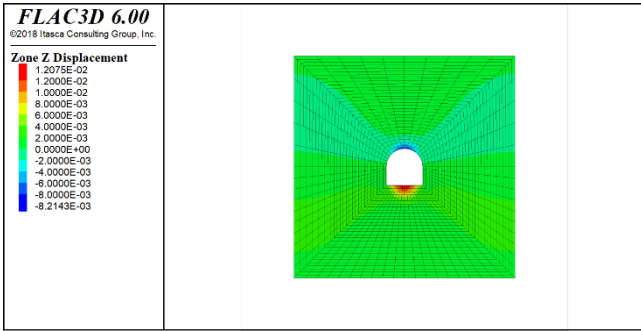


Figure 21. $\lambda=2.5$

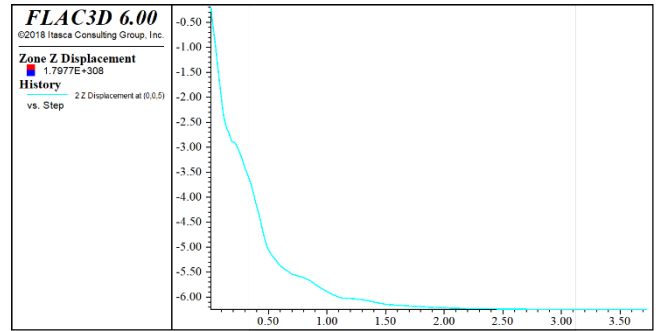


Figure 26. $\lambda=2$

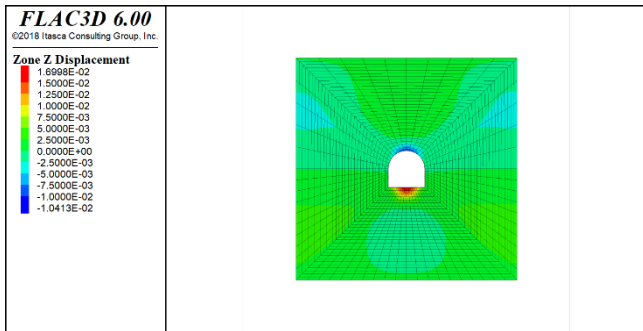


Figure 22. $\lambda=3$

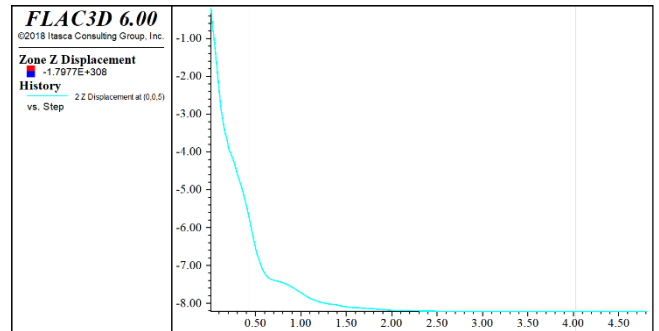


Figure 27. $\lambda=2.5$

The displacement curves in the Z direction of the vault after excavation with different lateral pressure coefficients are shown in the following figure:

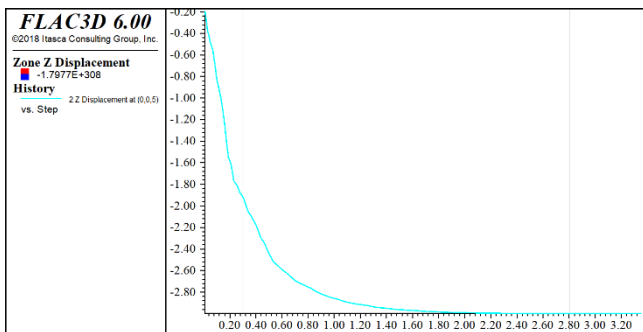


Figure 23. $\lambda=0.5$

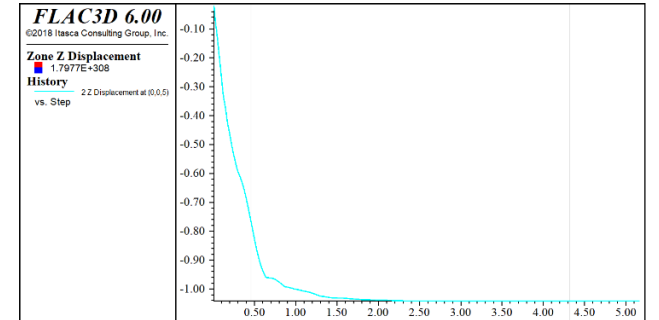


Figure 28. $\lambda=3$

The stress contour diagram in the Z direction after excavation with different lateral pressure coefficients is shown in the figure below:

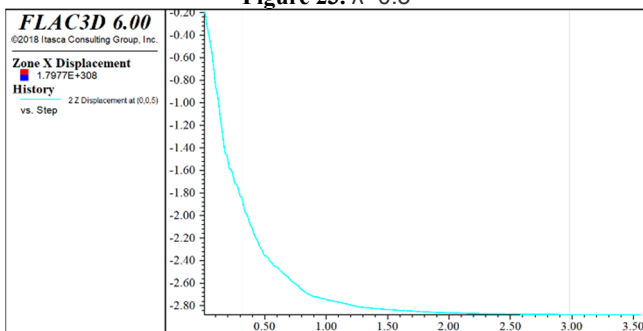


Figure 24. $\lambda=1$

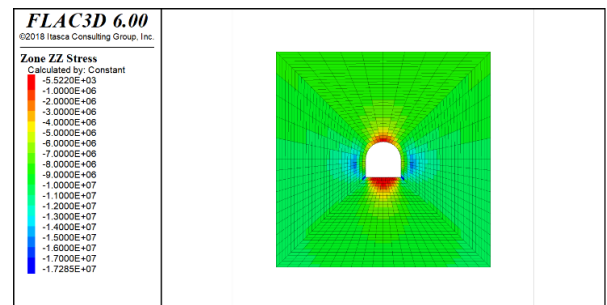


Figure 29. $\lambda=0.5$

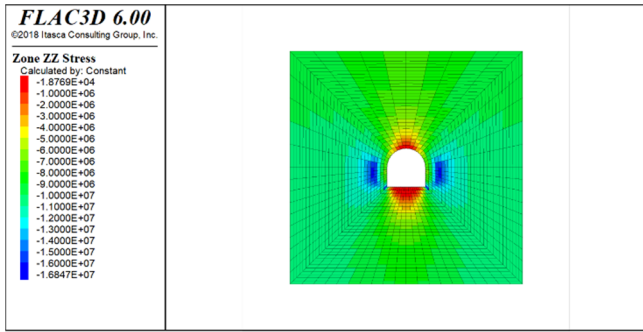


Figure 30. $\lambda=1$

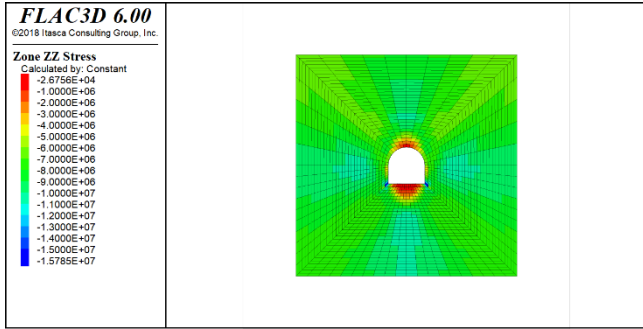


Figure 31. $\lambda=1.5$

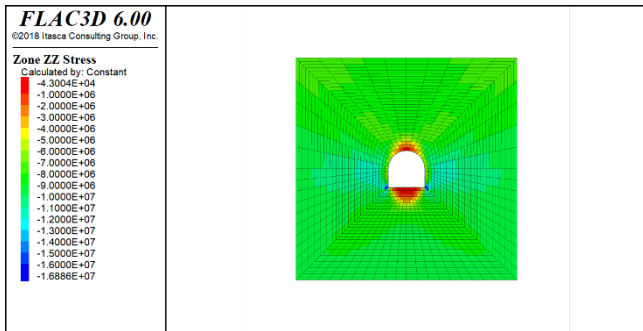


Figure 32. $\lambda=2$

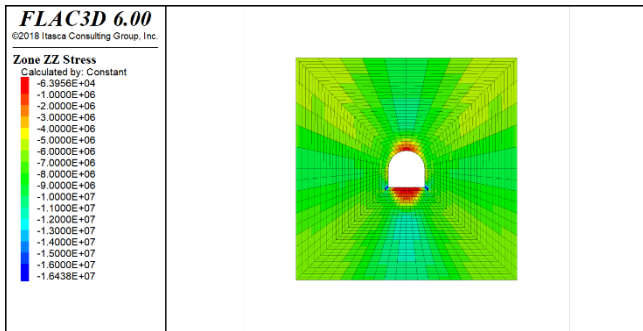


Figure 33. $\lambda=2.5$

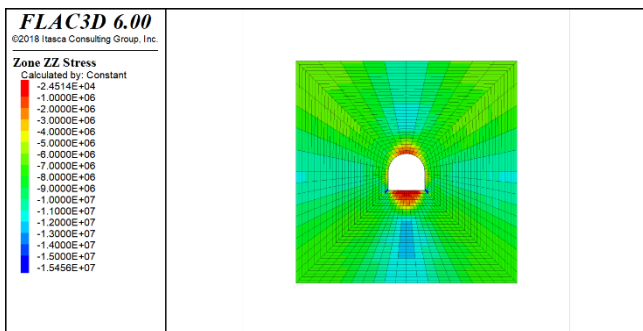


Figure 34. $\lambda=3$

shown in the figure below:

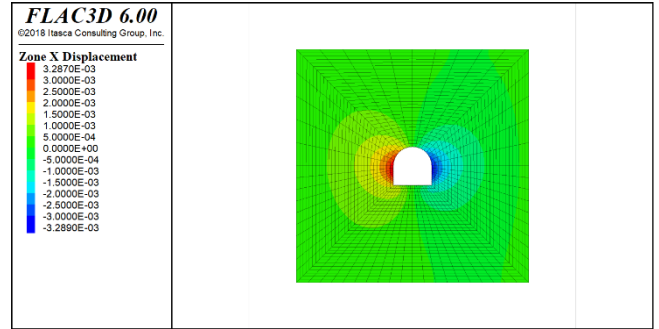


Figure 35. $\lambda=0.5$

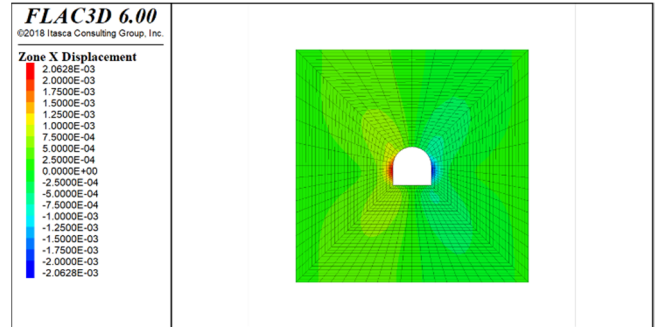


Figure 36. $\lambda=1$

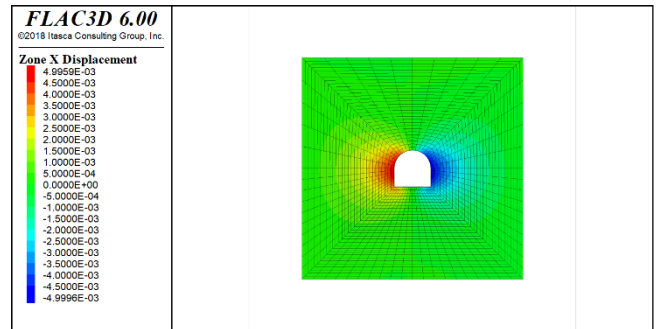


Figure 37. $\lambda=1.5$

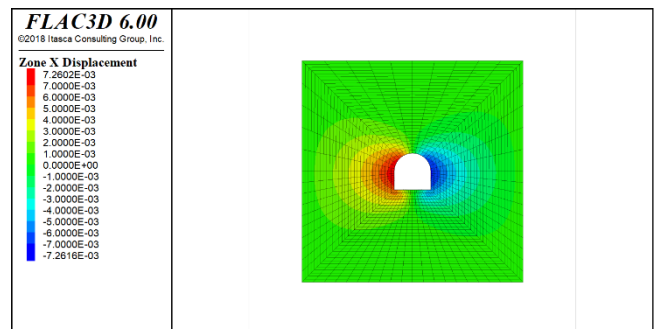


Figure 38. $\lambda=2$

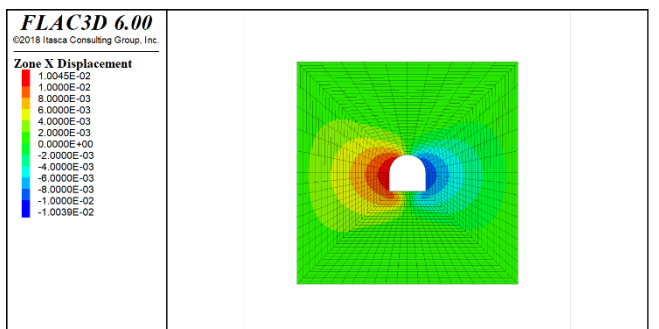


Figure 39. $\lambda=2.5$

The displacement contours in the X direction after excavation with different lateral pressure coefficients are

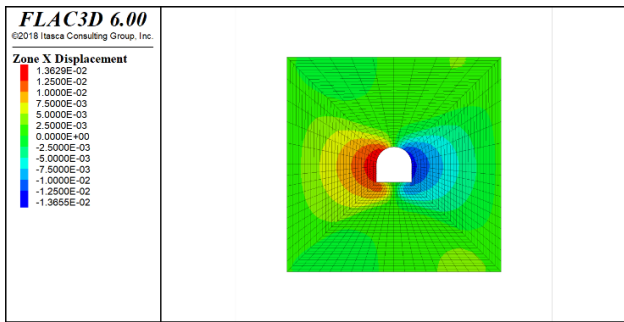


Figure 40. $\lambda=3$

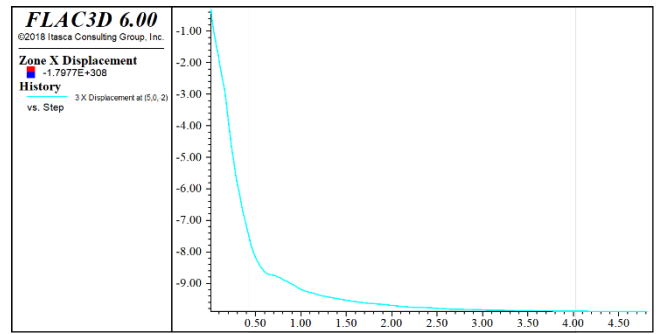


Figure 45. $\lambda=2.5$

The displacement curves in the X direction of the vault after excavation with different lateral pressure coefficients are shown in the figure below:

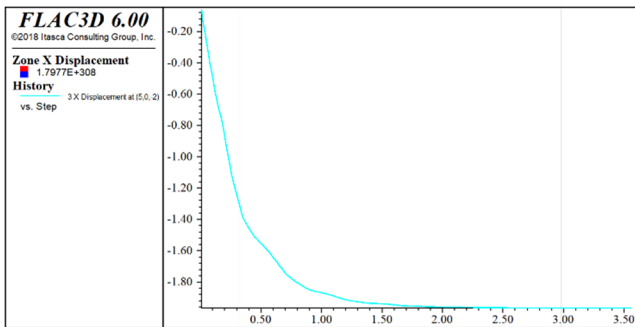


Figure 41. $\lambda=0.5$

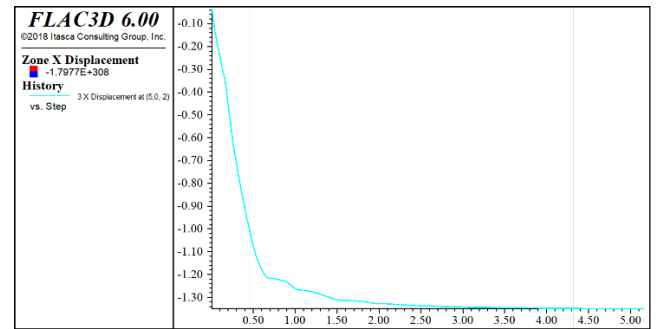


Figure 46. $\lambda=3$

The stress contour diagram in the X direction after excavation with different lateral pressure coefficients is shown in the following figure:

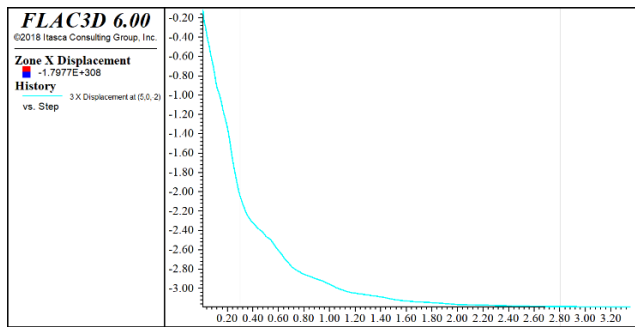


Figure 42. $\lambda=1$

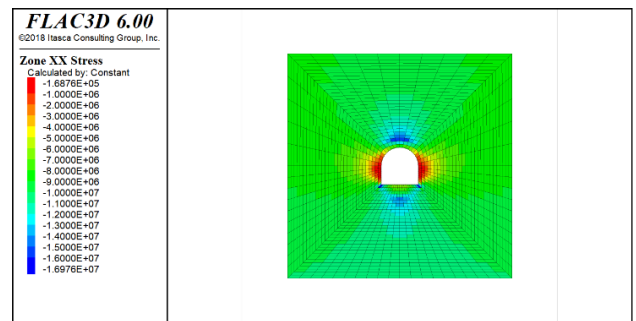


Figure 47. $\lambda=0.5$

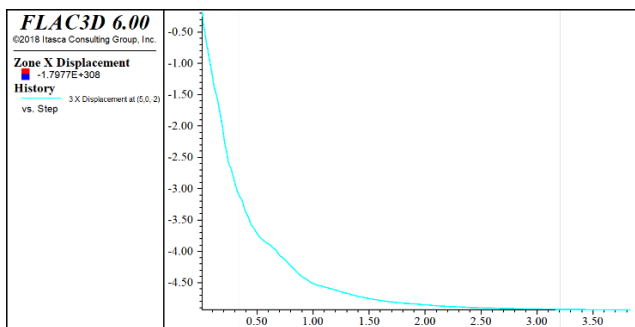


Figure 43. $\lambda=1.5$

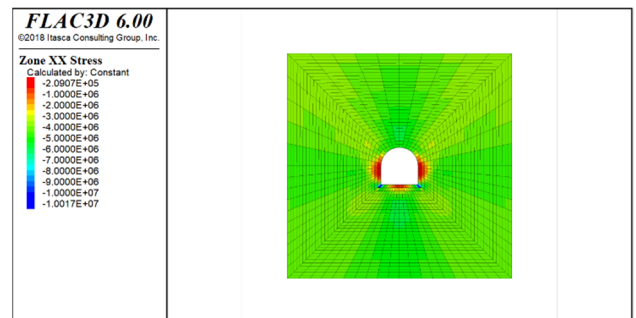


Figure 48. $\lambda=1$

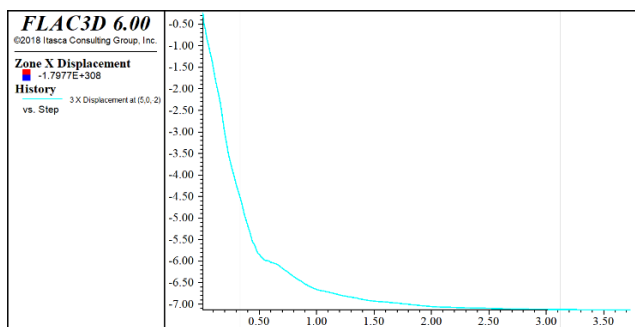


Figure 44. $\lambda=2$

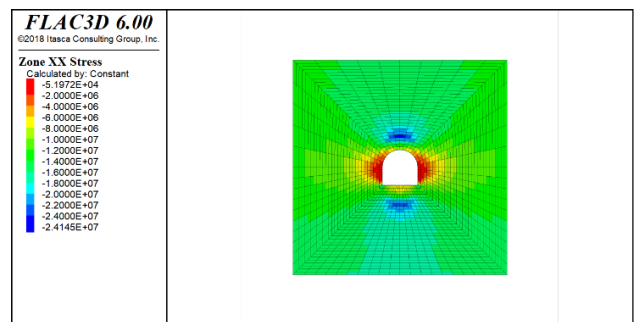


Figure 49. $\lambda=1.5$

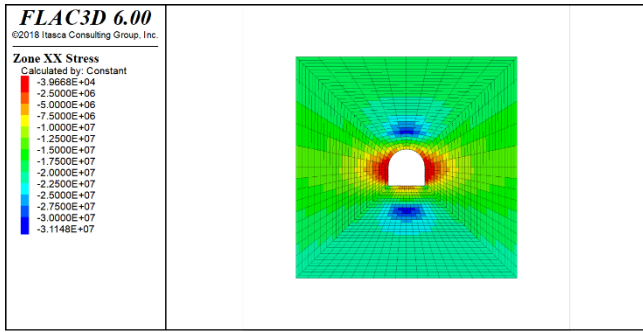


Figure 50. $\lambda=2$

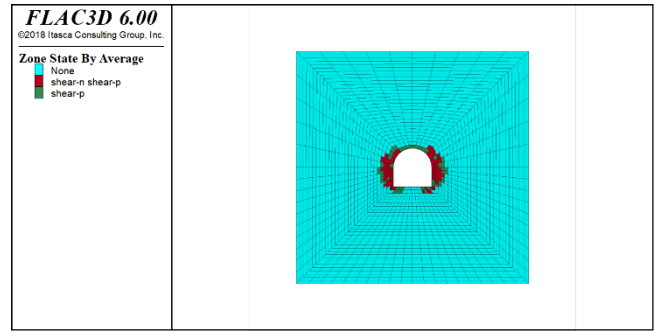


Figure 53. Plastic zone before support

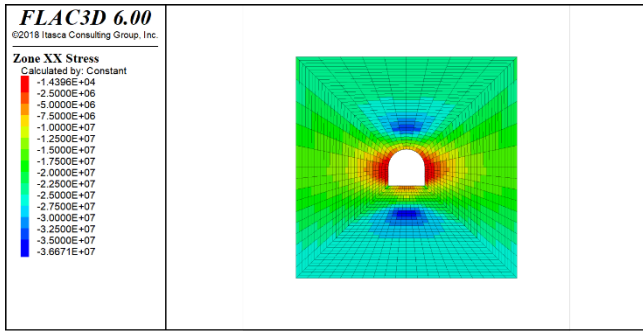


Figure 51. $\lambda=2.5$

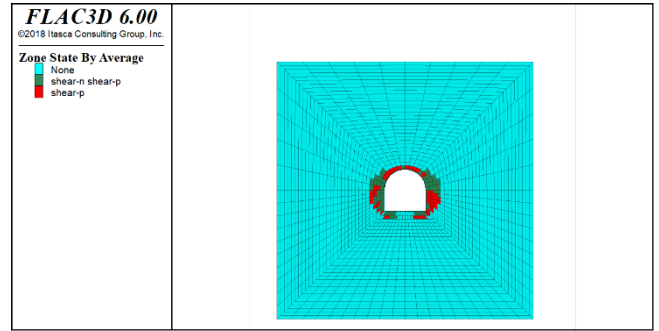


Figure 54. Plastic zone after support

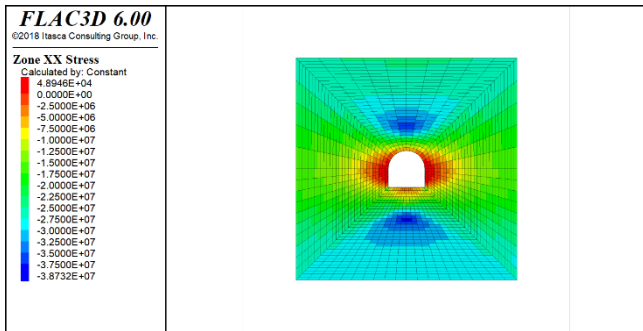


Figure 52. $\lambda=3$

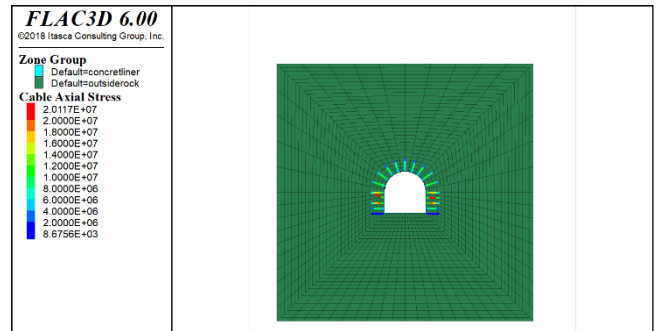


Figure 55. Stress of the bolt

It can be seen that with the increase of the lateral pressure coefficient, the vertical displacement of the vault and the horizontal displacement of the side wall increase correspondingly, and the horizontal displacement increases faster than the vertical displacement. The plastic zone increases with the increase of the lateral pressure coefficient, and the plastic zone at the vault increases more. This indicates that the horizontal tectonic stress has a great influence on the horizontal displacement of the side wall and the plastic zone of the vault.

Table 1. Statistical table

Lateral pressure coefficient (λ)	0.5	1	1.5	2	2.5	3
Vault vertical displacement (mm)	2.861	2.988	4.217	6.222	8.142	1.198
Horizontal displacement of side wall (mm)	2.052	3.253	4.949	7.200	9.963	1.319

5. Bolt Support After Tunnel Excavation

The calculation result after support is as follows:

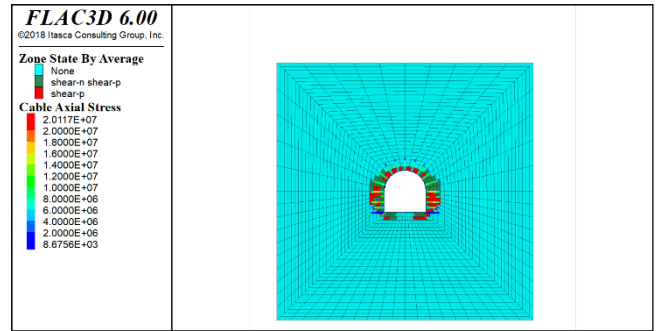


Figure 56. Relative position of the bolt and the plastic zone

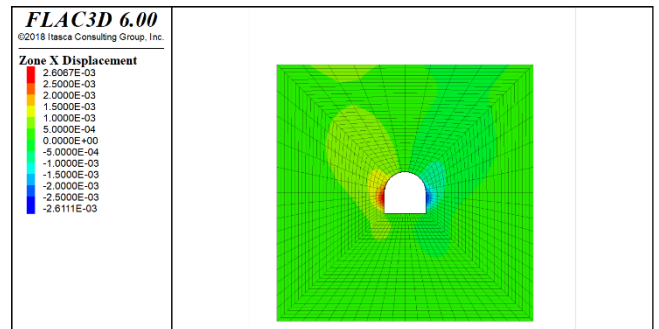


Figure 57. X-direction displacement contour after support

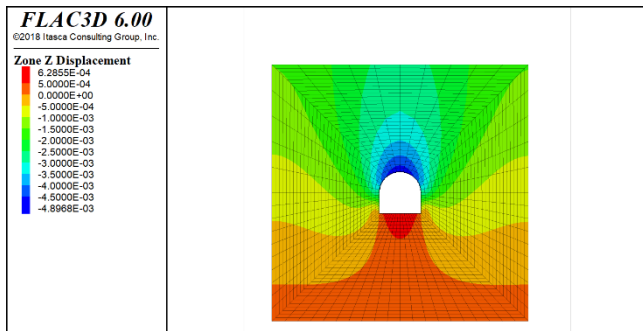


Figure 58. Z-direction displacement contour after support

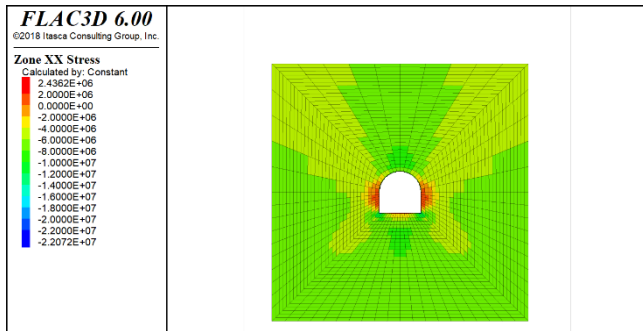


Figure 59. Stress contour in the X direction after support

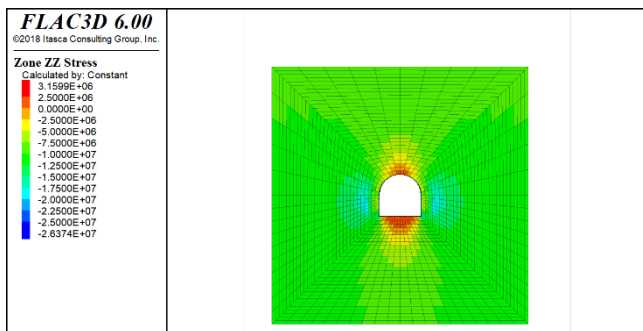


Figure 60. Stress contour in the Z direction after support

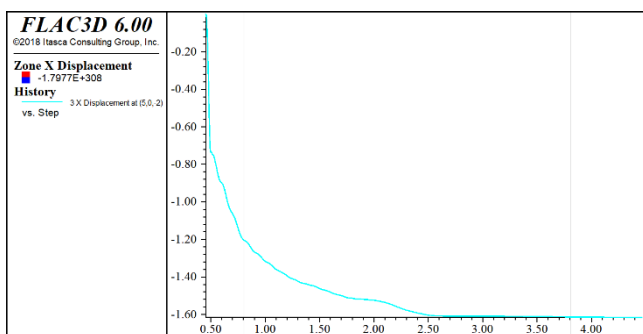


Figure 61. Displacement curve in X direction after support

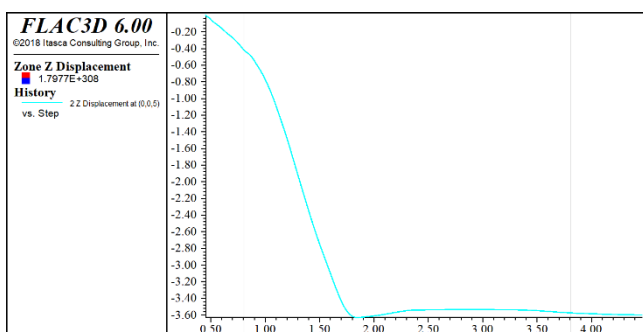


Figure 61. Displacement curve in Z direction after support

As can be seen from the figure, the plastic zone after

support is obviously much smaller than that without support, and the stress of the surrounding rock after support is improved, and the vertical displacement and horizontal displacement are reduced. A turning point can be clearly seen in the displacement curve, which is caused by the restriction of the deformation of the surrounding rock after the application of the initial support, which prevents the further deformation of the surrounding rock.

Table 2 Comparison table before and after support

	Vault vertical displacement X0 (mm)	Horizontal displacement of side wall Z0 (mm)
Pre-support	3.181	5.199
After supporting	1.622	3.625

6. Conclusion

After in-depth study of FLAC3D numerical simulation of tunnel excavation process, we draw the following conclusions:

(1) During tunnel excavation, the stress distribution of surrounding rock changes significantly. At the beginning of excavation, the stress concentration around the tunnel is obvious, especially at the top and bottom of the tunnel, there are relatively concentrated tensile stress and compressive stress. With the progress of excavation, the stress gradually tends to be stable, but there is still a phenomenon of stress concentration in some areas, and special attention should be paid to the support design in these areas.

(2) FLAC3D simulation results show that the surrounding rock has obvious displacement and deformation after tunnel excavation. Among them, the subsidence deformation at the top and bottom of the tunnel and the convergence deformation of the side wall are the main deformation forms. These deformations are affected by many factors, including geological conditions, excavation methods, support measures, etc. Through reasonable support design and construction scheme, the displacement and deformation of surrounding rock can be effectively controlled.

(3) Numerical simulation results show that the stress and displacement deformation of surrounding rock are effectively controlled after adopting reasonable support measures. The supporting structure can effectively share the stress of surrounding rock, reduce the phenomenon of stress concentration, and limit the displacement and deformation of surrounding rock. Therefore, in the process of tunnel excavation, it is very important to select the appropriate supporting structure types and parameters.

Based on the above conclusions, we suggest that geological conditions and construction conditions should be fully considered in the process of tunnel excavation, and appropriate excavation methods and support measures should be selected. At the same time, on-site monitoring and data analysis should be strengthened to discover and deal with possible safety hazards in a timely manner. In addition, the construction scheme and support design should be continuously optimized to improve the safety and economy of tunnel excavation.

References

- [1] LEI Gang. Research on FLAC~(3D) numerical simulation of excavation sequence of Dawangou Tunnel [J]. Journal of Geotechnical Engineering, 2014, 28(03): 81-83.

- [2] Xue Dandan. Simulation study on circular tunnel excavation under different working conditions [J]. Shanxi Metallurgy, 2021, 44(04): 14-1167/ Tp.2021.04.46.
- [3] You Fan-Fan, Qiu Xiaoli. Numerical simulation and analysis of tunnel step excavation based on FLAC3D [J]. Shanxi Architecture, 2014, 40(28):189-190.
- [4] TENG Haiwen, Wang Tao, Huo Yuhui, Hao Zhe. Three-dimensional stability analysis of Shenyang Subway tunnel excavation based on FLAC~(3D) [J]. Journal of Beijing University of Technology, 2009, 35(08):1074-1079.
- [5] Shao Jianguo. Numerical Simulation analysis of FLAC3D in tunnel construction [J]. Gansu Science and Technology, 2014, 30(23):130-133. (in Chinese)
- [6] PENG Kun, Tao Lianjin, Gao Yuchun, Wang Feng, Huang Jun. Numerical analysis of displacement of pile foundation caused by shield tunnel under bridge [J]. Chinese Journal of Underground Space and Engineering, 2012, 8(03):485-489.
- [7] Qin Lin. Analysis of the influence of tunnel excavation on the stability of mountain slope and study on strengthening measures [D]. Central South University, 2012.
- [8] Li Shuguang, Feng Xiaoling, Fang Ligang. Numerical Simulation of shield tunnel construction [J]. Standard Railway Design, 2009(03).1004-2954.2009.03.025.
- [9] Bao Hao, Zhou Xuhui, Ge Bin, Fang Chao. Key command flow of tunnel excavation based on FLAC3D [J]. Henan Science, 2019, 38(02):287-291. (in Chinese)
- [10] Lei Gang. Research on FLAC~(3D) numerical simulation of Dawangou Tunnel excavation sequence [J]. Geotechnical Foundation, 2014, 28(03):81-83.
- [11] Zhong Hao. Effect of tunnel excavation on slope stability based on FLAC~(3D) dynamic analysis [J]. Highway Engineering, 2010, 35(04):147-149+153.
- [12] LI Bingtian, Wang Peirong, Jin Feng, Dong Xu. Multi-arch tunnel excavation and support based on FLAC3D [J]. China Water Transport (Academic Edition), 2006(10):88-90.
- [13] Gou Yulong, Wang Honglong. Analysis of Tianzhushan Tunnel excavation and Stability evaluation of Supporting Structure [C]//. Proceedings of the 28th Annual Conference of Beijing Mechanical Society (II). [Publisher unknown], 2022. 2022.001631.
- [14] Cao Riyue. FLAC3D numerical analysis of a tunnel under different side pressure coefficients [J]. Journal of Taiyuan University of Science and Technology, 2016, 37(03):243-247.
- [15] Cao Riyue. FLAC3D numerical analysis of a tunnel under gravity stress field [J]. Home Industry, 2015(14):27-28.
- [16] Cheng Hao, Hu Xing. Treatment effect analysis of a karst tunnel support structure [J]. Journal of Guizhou University (Natural Science Edition), 2016, 33(03).2016.03.29.